Earthquake Geotechnical Engineering for Protection and Development of Environment and Constructions – Silvestri & Moraci (Eds)
© 2019 Associazione Geotecnica Italiana, Rome, Italy, ISBN 978-0-367-14328-2

1-g shaking table test study of the impact of repeated liquefactions

E. Baboz
University of Tokyo, Japan
ENPC, Marne-la-Vallée, France
K. Watanabe & J. Koseki
University of Tokyo, Tokyo, Japan

ABSTRACT: Soil liquefaction is one of the main concerns when assessing the potential damages of an earthquake. Several parameters have already been widely studied in terms of influence on the resistance against liquefaction of structures in sandy soil. However the effect of repeated liquefactions on the soil still remains unclear. In this study, saturated shaking table models were prepared with medium dense to dense silica sand and with a superstructure to investigate this impact. Two series of tests were compared: models ground were prepared with no liquefaction history before the structure installation as opposed to model grounds which were already subjected to repeated liquefaction stages before the structure installation. For both series, the mechanisms occurring during liquefaction appeared to be identical. However, in the case with model with liquefaction history, the damages were limited but also worsen in one case.

1 INTRODUCTION

Recent earthquakes such as the 2011 great East Japan earthquake or the 2010-2011 Christchurch earthquakes in New Zealand (Cubrinovski et al. 2012) caused extensive damages to structures through soil liquefaction. It appeared that liquefaction took place several times in the same area with more damages during the liquefaction event. As many areas with direct human activity have a high seismic activity, the problematic of repeated liquefaction is to be taken seriously.

The effect of strain history on liquefaction resistance was first observed by Finn et al. (1970) in laboratory tests. Large strain of the soil resulted in a reduction of the liquefaction resistance while small strain or partial liquefaction would increase it. In 2001, Oda et al. linked this impact to the induced anisotropy of the soil microstructure. The evolution of the microstructure of the soil through liquefaction was also investigated by Wang & Wei (2016) with the discrete element method. They observed that after the application of a large strain, the soil could display highly anisotropic particle-void structure and load-bearing capacities. This work focuses on the assessment of the soil performances on terms of liquefaction resistance and deformations for soils with history of liquefaction. In this study, physical models were prepared with medium dense to dense silica sand to investigate this impact on a 1-g shaking table apparatus.

The model tests were divided into two types of tests. In the first type, the model ground was prepared with no liquefaction history before the installation of the structure. In the second series, the model ground was subjected to repeated liquefaction stages before the structure installation. To quantify the differences of the two types of configuration, the excess pore water pressure generated in the soil, the response acceleration, as well as the displacement of the soil and the structure, were measured during the shaking table test.

2 TESTING PROCEDURE

2.1 *Test material*

The shaking table of the geotechnical laboratory of University of Tokyo was used to realize a series of model test. The models were prepared in a soil container mounted on a shaking table of 3m by 2m. The container was a rectangular box measuring 282cm in length, 40cm in width and 80cm in height. The acrylic panels on the sides allow for the observation of the soil during the test. Three types of sensors were used and installed in the model tests: accelerometer transducers pore water pressure transducers and laser sensors, as shown in Figure 1. In addition, four burettes were connected to the side of the soil container in order to check the water table in the model. The soil properties of the silica sand used for the tests are listed in Table 1.

2.2 *Preparation procedure*

The transducers were heavier than the surrounding sand and would have settled significantly if used as is. As fixing the sensors with wires would have reinforced the soil, the author chose to adjust the overall unit weight of the sensors to match the saturated unit weight of the sand ($\approx 18 kN.m^{-3}$). This was done by adding a small volume of Expanded Polystyrene to the sensors, as it has the advantage of being an extremely light material.

In order to prepare the ground model to the intended density, the method of air pluviation has been chosen. A manually operated sand hopper was used for this procedure and by this method the author was able to achieve the target density of the soil. The parameters impacting

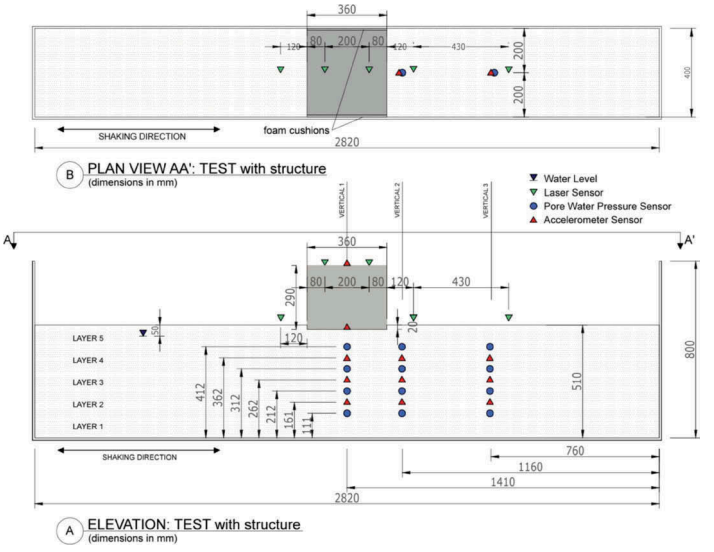

Figure 1. Model test layout after installation of the superstructure.

Table 1. Soil properties.

Soil	Specific gravity Gs	e_{min}	e_{max}	Mean particle diameter, D_{50}	Effective particle diameter, D_{10}	Coefficient of uniformity, Uc	Coefficient of curvature, U'c
Silica sand n.7	2.64	0.670	1.129	0.170 mm	0.110 mm	1.855	0.945

the obtained density of the sand in the model were: the velocity of the top container from which the sand is falling, the rate of the sand flow, controlled by the opening size of the hopper, and the falling height of the sand.

The saturation of the soil was done from the bottom using five water inlets connected at the base of the container. During the model preparation, the saturation speed was carefully controlled. This monitoring was done in order to avoid the following issues: if the saturation was too slow, it could lead to the creation of unsaturated zones caused by the suction of the upper part of the model. A reduction of the degree of saturation increases the resistance against liquefaction and would affect the test results. On the other hand, if the saturation was too fast, it could lead to local collapses of the model ground. To avoid such issues, the water saturation of the model was made with a constant pressure of 3kPa. For this study, the saturation of all tests has been done with normal water (no vacuuming) and without pre-application of carbon dioxide. After the water head reached the soil surface, the level was lowered by 5cm.

The preparation of the physical model was made by scaling down a 6-story building by a factor of 20. Rocking motion could occur during the dynamic loading but was not the interest of this study; therefore the height of the model was limited to 25cm. This type of structure has been chosen for the tests due to its relatively simple set up procedure.

2.3 *Application of seismic load*

The input motion for the model tests applied is 20 uniform sinusoidal cycles with a shaking duration of 4 seconds, therefore corresponding to a shaking frequency of 5Hz. By taking this shaking frequency, the model was shaken far from the natural frequency of the soil.

Table 2 below summarizes the series of tests carried out in the scope of this work. The tests have been separated into two groups of similar initial density (after structure installation): Group I (D_r = 89%) and Group II (D_r = 70%).

Test 2, Test 4 and Test 5 have been split in two parts: the phase A and the phase B that were performed continuously on the same ground model.

The part A corresponds to the model ground shaking history in which several liquefaction events took place. During this phase, no structure was installed on the ground. This simulates the soil history.

The part B corresponds to the shaking phase on the model ground once the structure was installed: a 36cm x 36cm wooden box of 40kg. Its loading phase was identical with the one of Test 1 and Test 3.

Table 2. Relative density and test parameters for all tests.

Group	Name of tests	Relative density	Structure	Amplitude if the input acceleration	Note
I	Test 1	89%	Box – 40kg	800cm.s^{-2}, 900cm.s^{-2}, 1000cm.s^{-2} x12	With structure
	Test 2-A	40%	/	400cm.s^{-2} x 14, 500cm.s^{-2}, 600cm.s^{-2}, 700cm. s^{-2}, 800cm.s^{-2} x2	Shaking History
	Test 2-B	89%	Box – 40kg	800cm.s^{-2}, 900cm.s^{-2}, 1000cm.s^{-2} x12	With structure
II	Test 3	70%	Box – 40kg	800cm.s^{-2}, 900cm.s^{-2}, 1000cm.s^{-2} x12	With structure
	Test 4-A	40%	/	400cm.s-2 x5	Shaking History
	Test 4-B	70%	Box – 40kg	800cm.s^{-2}, 900cm.s^{-2}, 1000cm.s^{-2} x12	With structure
	Test 5-A	40%	/	400cm.s-2 x6, 300cm.s-2 x2, 200cm.s-2 x1, 100cm.s-2 x 6	Shaking History
	Test 5-B	70%	Box – 40kg	800cm.s^{-2}, 900cm.s^{-2}, 1000cm.s^{-2} x12	With structure

The relative densities at the beginning of the phase B were determined by considering the grounds settled homogeneously and by measuring the model settlement at the soil surface at the end of the phase A.

2.4 *Analysis methodology*

For this research, the sampling frequency of 500Hz was chosen with the data acquisition duration of 98 seconds. The data was processed per the following formulas, following the following method (Koga & Matsuo 1990):

$$\tau = \sum m.a \tag{1}$$

Where τ is the shear stress, m the mass of the soil and a the horizontal acceleration.

$$\gamma = \Delta d/\Delta h \tag{2}$$

Where γ is the shear strain, d the displacement measured by two horizontally consecutive accelerometers and h the height difference between these accelerometers.

$$\sigma_\nu = H_{soil} \cdot \gamma_{soil} \tag{3}$$

$$u = H_{water} \cdot \gamma_{water} \tag{4}$$

Where σ_ν is the initial vertical stress and u is the pore water pressure, both before application of the dynamic load. H_{soil} is the overlying soil height, γ_{soil} is the soil unit weight, H_{water} is the water head and γ_{water} is the water unit weight.

$$\sigma'_\nu = \sigma_\nu - u \tag{5}$$

Where σ'_ν is the effective vertical stress. The excess pore water pressure ratio, R_u, was calculated as per the following formula (Koga & Matsuo 1990):

$$R_u = \Delta u/\sigma'_\nu \tag{6}$$

In addition, the double amplitude in shear strain, γ_{DA}., has also been taken as a criterion in order to assess the liquefaction resistance of a ground model under repeated input acceleration. The target double amplitude value for this work has been taken as 1.5%. For each cycle, the double amplitude of the shear strain is calculated. This value is compared to the criteria (1.5%). Once the value exceeds the criteria, the number of cycle N_γ is calculated by interpolation between the exceeding value of the double amplitude in shear strain, $Y_{DA(Ni+0.5)}$, and the previous value, $Y_{DA(Ni)}$, calculated as per the formula in Equation 7:

$$N_\gamma = \left(0.5 * (1.5 - Y_{DA(Ni)})/(Y_{DA(Ni+0.5)} - Y_{DA(Ni)})\right) \tag{7}$$

For this study, the data from the accelerometer were integrated twice with the Newmark-β method using the following parameters: γ = ½ and β = ¼. In order to minimize any potential drift due to the integration of recorded noise and offset, the signal is processed through a fast-Fourier transform high pass filter with a cut-off frequency of 2Hz before each integration step. By choosing this cut-off frequency, the data were not altered. The equations used were:

$$\dot{u}_{i+1} = \dot{u}_i + (1-\gamma).\Delta t.\ddot{u}_i + \gamma.\Delta t.\ddot{u}_{i+1} \tag{8}$$

$$u_{i+1} = u_i + \Delta t.u_i + (0.5-\beta).\Delta t^2.\ddot{u}_i + \beta.\Delta t^2.\ddot{u}_{i+1} \tag{9}$$

Where u is the displacement. By taking the initial condition of zero for the displacement and velocity, it is possible to calculate step-by-step the velocity and displacement for each accelerometer.

3 TEST RESULTS AND DISCUSSION

3.1 *Deformation*

The deformation occurring after the structure was installed was measured by taking the mean value between two laser sensors attached above the structure (Figure 1). Even though the model was subjected to several shaking steps, the author focused on the structure subsidence of the first stage since the ground models' relative densities were comparable. The deformation occurring following the first shake on the model with structure is shown Figure 2.

For Group I (with a model initial density of 89%) the ratio of subsidence recorded was of 2:1 (14mm/7mm) between Test 1 and Test 2 as shown in Table 3. The liquefaction history seemed to have reduced the subsidence mechanism of the sand surrounding the superstructure.

For Group II (with a model initial density of 70%), the results did not display a single trend. As shown in Table 3, the ratio was of 1:1.6 between Test 3 and Test 4 (40mm/65mm). Therefore, it seems that the liquefaction history had a negative effect on liquefaction resistance of the ground model for Test 4. However, similarly as for Group I, the ratio was of 2.4:1 (40mm/17mm) between Test 3 and Test 5. The liquefaction history had a positive impact on the liquefaction resistance of the ground model of Test 5.

3.2 *Model's response during the first shake for model ground with structure*

It appeared that the relative density had an impact on the subsidence occurring during the liquefaction of the model ground. However, in some cases, the repeated liquefactions that happened in the cases with liquefaction history had a non negligible impact on the liquefaction induced

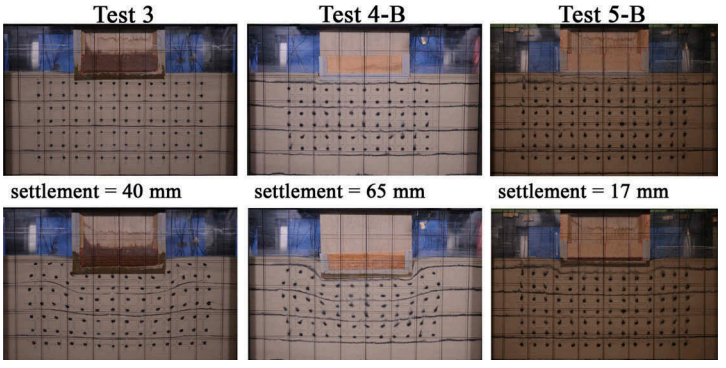

Figure 2. Deformation occurring following the first shake on the model with structure for Test 3, Test 4-B and Test 5-B.

Table 3. Comparison of the structure subsidence for the first shake on the model with structure.

Group	Name of tests	Subsidence* at the 1st shaking	Tilting angle	Liquefaction history	Note
I	Test 1	14 mm	0.1°	No	
	Test 2-B	7 mm	0.2°	Yes	More resistance to deformation
II	Test 3	40 mm	0°	No	
	Test 4-B	65 mm	2.7°	Yes	Less resistance to deformation
	Test 5-B	17 mm	0.1°	Yes	More resistance to deformation

* The subsidence was calculated as the mean value of two displacement values measured by the laser sensors (in Figure 1 is shown the measurement locations).

Table 4. Summary of the model's response during the 1st shaking with structure installed.

Name of tests	Subsidence at the 1st shaking	Max Ru generated during the 1st shaking	Max acceleration recorded at the base of the box (g)	Max acceleration recorded at the top of the box (g)
Test 1	14 mm	0.18	1.15	1.15
Test 2-B	7 mm	0.45	2	1.8
Test 3	40 mm	0.35	/	1.2*
Test 4-B	65 mm	0.55	1.2*	1.2*
Test 5-B	17 mm	0.6	1	1

* Acceleration at first cycle, then severely reduced in small cycles < 0.25g

mechanism around the structure during what is called the first shaking of phase B (first dynamic load applied once the structure is set in the model). The results are summarized in Table 4.

However, a trend was observed with the dynamic response of the structure. The most important subsidence of the box appeared to be associated with a very important damping of the structure, which could be measured with the top and bottom accelerometers as shown on Figure 1. As shown in Figure 3, the Test 3 and the Test 4-B, the accelerometers of the box recorded an initial peak very important, around 1.2g. However, directly from the second peak, the acceleration recorded was greatly reduced and stayed under 0.25g.

3.3 *Strain history and liquefaction resistance of the model before the structure installation*

It has been previously observed that even though Test 4-B and Test 5-B had the same initial density, the ground behavior under the liquefaction of the first shake was very different. It has

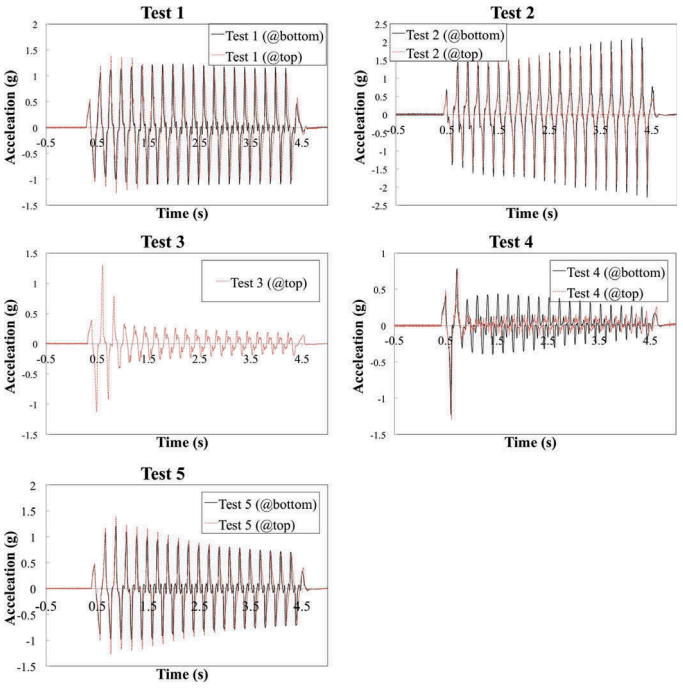

Figure 3. Acceleration measured at the top and bottom of the superstructure (Test 1 to Test 5).

been noted in previous works (Finn et al. 1970, Wahyudi et al. 2015) that the strain history of a soil has an important effect on its liquefaction resistance. Therefore, to investigate further the differences observed in terms of deformation between the tests with liquefaction history, the maximum double amplitude of the shear strain was calculated and compared between the different histories. The results are shown in Figure 4, in which are displayed the values for Test 2-A, Test 4-A and Test 5-A.

Test 2-A, Test 4-A and Test 5-A began with the same loading protocol (although Test 5-A had a small accidental shock counted as Shake N.2 which was negligible). The strain in all three tests has the same trend of evolution. When Test 4-A was stopped, it corresponded to a critical point. In Figure 4, it appears that the last shaking of the model ground corresponded to a high value of shear strain: about 10% of double amplitude. In Figure 5, it also appears that it corresponds to a low value of liquefaction resistance. The gradual increase of the maximum γ_{DA} stage by stage could have resulted in a possible anisotropy of the ground model. On the other hand, the liquefaction history of Test 5-A was done in a decreasing manner, as described in Table 2. It started at an input acceleration of 400cm.s-2 and was, later on, decrease to 300cm.s-2, followed by 200cm.s^{-2} and ultimately 100cm.s^{-2}. It can be seen, Figure 4, that the last input motion induced very small values of γ_{DA}. γ_{DA} was kept under 0.1%. According to the findings of Wahyudi et al. (2015), small strain significantly increased liquefaction resistance. Therefore, the small strain history of Test 5-A can be at the origin of the positive effect on phase B with the superstructure.

However, in the case of Test 2-A, the ground seem to be subjected to very important shear strain, as shown in Figure 4, and its liquefaction resistance seems to be decreasing in Figure 5.

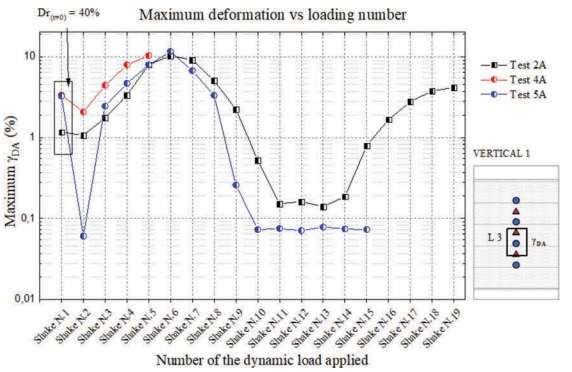

Figure 4. Maximal double-amplitude of the shear strain measured in the ground model vs. the nth dynamic load applied on the model.

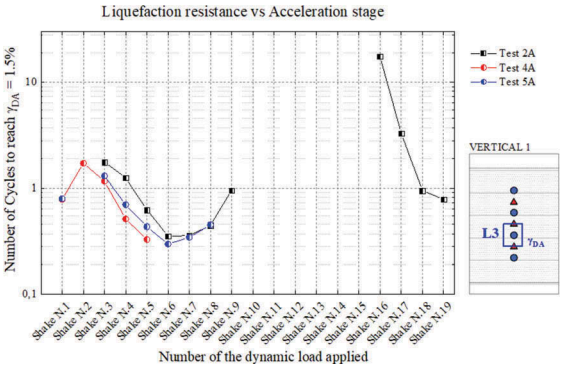

Figure 5. Liquefaction resistance of the model (N_γ) vs. the nth dynamic load applied on the model.

This observation does not seem to be in accordance to the previous result in deformation that showed that the subsidence was reduced for Test 2-B.

4 CONCLUSION

A series of 1-g shaking table tests were performed with a small-scale model with the aim to evaluate the effect of repeated liquefaction on further liquefaction induced mechanism of building subsidence. In regards to the tests results and comparison with similar studies, several conclusions can be drawn:

1. The application of a liquefaction history had an impact on the performance of a structure subjected to strong shakings.
2. During this study, the effects of liquefaction history observed could be positive but they could also be negative as in one case the structure appeared to have subsided more.
3. The effects of liquefaction history appeared to be linked to the strain history that occurred before the superstructure installation.
4. The relative density of the ground model also played an important role in terms of structure subsidence, but in some cases, it can be significantly minimized by liquefaction history.
5. In one case, the strain history did not seem to be consistent with an increased liquefaction resistance. The reason behind this remains unclear and would need further investigation.

ACKNOWLEDGEMENT

This work was supported by the Monbukagakusho scholarship granted by the government of Japan. The authors acknowledge the financial support. In addition, we thank the Ecole National des Ponts ParisTech for allowing the academical exchange and the University of Tokyo for providing an excellent research environnment. We wish to thank also the following persons: Hiroyuki Kyokawa, Yuya Nakade, Takeshi Sato, Jean-Claude Dupla, Massimina Castiglia, Loric Renault, Kebba Trawally and Zafar Avzalshoev who greatly assisted the research.

REFERENCES

Cubrinovski, M., Henderson, D. & Bradley, B. 2012. Liquefaction impacts in residential areas in the 2010-2011 Christchurch earthquakes. *Proc. of International Symposium on Engineering Lessons Learned from the Giant Earthquak*: 811–824.

Finn, W.D.L., Bransby, P.L. & Pickering, D.J. 1970. Effects of strain history on liquefaction of sands. *Proc., ASCE*, 96(6): 1917–1934.

Koga, Y. & Matsuo, O. 1990. Shaking Table Tests of Embankments Resting on Liquefiable Sandy Ground. *Soils and Foundations* 30(4): 162–174.

Oda, M., Kawamoto, K., Suzuki, K., Fujimori, H. & Sato, M. 2001. Microstructure interpretation on reliquefaction of saturated granular soil under cyclic loading. *Journal of Geotechnical and Geoenvironmental Engineering*, 127(5): 416–423.

Teparaksa, J. 2017. *Comparison of sand behavior under liquefaction in triaxial and shaking table tests (PhD dissertation)*. Tokyo: University of Tokyo.

Wahyudi, S., Koseki, J., Sato, T. & Chiaro, G. 2015. Multiple-liquefaction behavior of sand in cyclic simple stacked-ring shear tests. *International Journal of Geomechanics*, 16(5).

Wang, G. & Wei, J. 2016. Microstructure evolution of granular soils in cyclic mobility and post-liquefaction process. *Granular matter*, 18(3).